

In-vivo Lung Cancer Imaging in Mice using 360° Free-space Fluorescence Molecular Tomography

Nikolaos Deliolanis, Tobias Lasser, Mark Niedre, Antoine Soubret and Vasilis Ntziachristos

Abstract—We present the development and performance characteristics of a free-space fluorescence tomography system. The imaging system can capture complete angle projections of photons propagating through tissue in transillumination using a CCD camera. Experimental data on imaging lung cancer are presented. Overall, this imaging approach can offer unprecedented imaging performance in Fluorescence Molecular Tomography of small animals.

I. INTRODUCTION

FLUORESCENCE MOLECULAR TOMOGRAPHY (FMT) has a great potential to serve as investigational tool for small animal research and drug discovery. FMT comes to improve on several shortcomings of planar epi-illumination methods that use CCD cameras to image fluorescence back-emitted from tissues after wide-field illumination. The method is based on tomographic principles, coupled to the use of appropriate models of photon propagation in tissues [1-5] and can offer significantly improved imaging ability and quantification since it can resolve depth and account for the heterogeneous attenuation of light intensity by tissues, due to the variation of the optical properties.

In this paper we present advances associated with the development of a new generation of system that enables high spatial sampling of photon fields propagating through tissues at 360° projections. The principle of operation is based on the use of non-contact laser illumination scanned on one side of the diffusive object or animal and of CCD cameras for photon detection. This approach operates in the absence of fibers or matching fluids and significantly improves experimental procedures and the collection efficiency. The feasibility of using non-contact measurements in FMT has been shown recently [6-9]. In this invited talk we demonstrate the combination of surface extraction and 360° projection data to tomographically imaging molecular signatures in small animals in the near-infrared. In particular we discuss the imaging scanner and the basic theoretical mainframe to achieve 360° free-space fluorescence molecular tomography and showcase examples from phantoms and animal models of lung cancer.

Manuscript received April 3, 2006.

The authors are with the Laboratory for Bio-optics and Molecular Imaging at the Center for Molecular Imaging Research at the Massachusetts General Hospital and Harvard Medical School, CNY 149 13th street r.5209, Charlestown MA 02129. The e-mail of the corresponding author is vasilis@helix.mgh.harvard.edu.

II. THEORY

Tomographic reconstruction of fluorochrome distributions is based on the normalized Born approximation [5], which calculates the ratio of the measured fluorescence intensities $U_{\text{fluo}}(r_s, r_d)$ over the measured intrinsic intensities $U_0(r_s, r_d)$ at source position r_s and detector position r_d ,

$$U^{nB}(r_s, r_d) = \frac{U_{\text{fluo}}(r_s, r_d)}{U_0(r_s, r_d)}. \quad (1)$$

Correspondingly, a forward model is calculated to predict photon propagation in a diffuse medium by deriving appropriate weight (sensitivity) functions for each virtual source-detector pair employed. The resulting weight matrix is then inverted with a randomized algebraic reconstruction technique (R-ART) algorithm [10]. The advantage of using the normalized expression in (1) is that it eliminates position-dependent contributions and minimizes the sensitivity of the reconstruction to background heterogeneities.

To achieve an accurate photon propagation model in tissue it is important to capture the three-dimensional animal surface that bounds the diffusive tissue. The 3D surface reconstruction is done via volume carving [11] using the contours of the object after appropriate back-illumination using a photo-luminescent plate inserted behind the animal, on the opposite side of the CCD camera. The contours are acquired using our FMT scanner at 72 projections and are segmented via an adaptive thresholding algorithm. Using volume carving, an approximation to the real object is

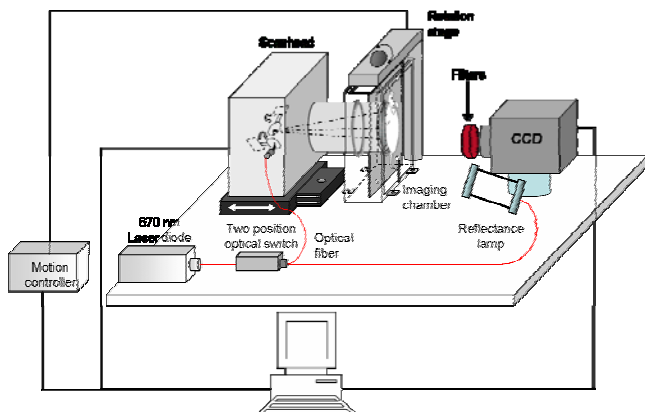


Fig. 1. Schematic of experimental setup for 3D surface reconstruction and FMT.

computed, the Visual Hull [12]. The resulting 3D model is

then meshed to a regular spaced grid and the surface is computed via a Marching Cubes type algorithm [13].

III. EXPERIMENTAL SETUP

The schematic of non-contact 360° rotation FMT system is shown in Fig. 1. It consists of a continuous laser diodes at 665nm and 748nm wavelengths coupled to an optical fiber through appropriate switches. The light beam is collimated and delivered to a two mirror scanhead system that can xy translate and focus the beam on the object [14]. A high-sensitivity CCD camera is placed in the opposite direction to record the light transmitted (or generated) through the object. The object is back-illuminated by a source pattern generated by the scanhead and the CCD camera records the transmitted field for every source. The object is mounted on a step-motor controlled rotating stage so that it can be illuminated from every direction and allowing for the acquisition of multiple projections. The rotation is also used to reconstruct the surface of the object from the contours of deferent projections when it is imaged against a homogenous illuminating background [15]. The intrinsic field that is transmitted and the fluorescence field generated in the object are recorded with the use of appropriate interferometric filters. The entire experiment procedure is completely automated and driven by a custom developed C program. Typical acquisition times for a 21 source and 15-projection experiment are 15min and the reconstruction time 1-2 min.

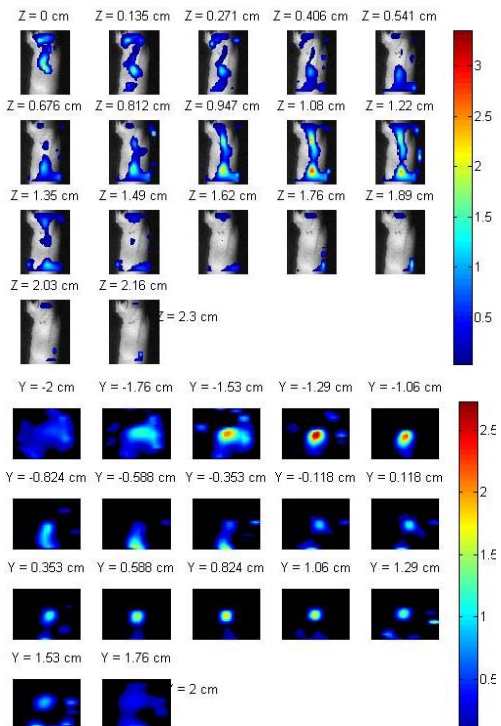


Fig. 4. Sagittal and axial sections of the reconstruction of the lung tumor.

A. Experimental measurements

To examine basic imaging feasibility in 360° free-space acquisition we performed phantom and in-vivo measurements. Typically, the surface capture accuracy was found to be better than 150 microns. For image reconstruction, 15 projections were employed (24 deg step) and a source scan pattern of a 7 x 3 grid over a 2 x 0.5 cm² area respectively. The acquired data were inverted by R-ART after 20 iterations.

For in-vivo measurements an in-vivo mouse model of lung cancer was employed. The study was performed according to the procedures approved by the Massachusetts General Hospital. The mouse was injected with 1×10^6 Lewis Lung Carcinoma (LLC) cells intra-coastally in the right lung. After 7 days the mouse was injected with 2 nmols of Angioscience680 (Visen Medical) via tail vain injection to image vascularization and permeability and it was imaged 18 hours later. During the experiment the mouse was anesthetized. Preliminary imaging results are presented in Figs. 2 and 3. The images show two areas of increased fluorescence concentration, one that is congruent with the location of the liver and one that is higher in the animal in the upper lung area, consistent with the location of tumor implantation.

IV. DISCUSSION-CONCLUSIONS

Free-space 360° FMT has the potential to offer unprecedented performance over slab geometry systems or fluid-based or fiber-based systems. In this talk we present key methodological aspects and results from mouse imaging in regard to this new imaging approach. We currently validate in-vivo imaging results with correlative anatomical

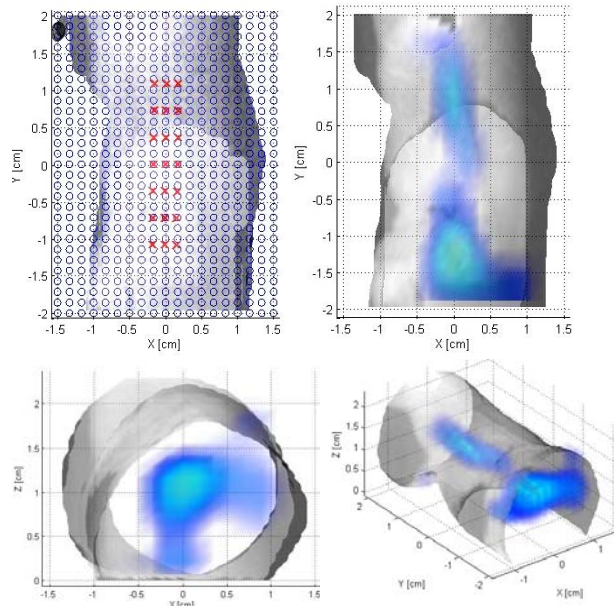


Fig. 5. 3D of the reconstruction of the lung tumor. Geometry of the source pattern and the virtual detectors, and 3D views of the reconstructions.

imaging and histological evaluations. Based on these results we can further optimize the system design and parameters of operation for facilitating optimal imaging performance. In the future we expect to extend the applications of this technology to other animal models and the use of more elaborate fluorescence reporter technologies.

ACKNOWLEDGMENT

The authors acknowledge support from NIH grant ROI EB000750-1 and R43-ES012360.

REFERENCES

- [1] X.D. Li, M.A. Oleary, D.A. Boas, B. Chance, and A.G. Yodh, "Fluorescent diffuse photon: Density waves in homogeneous and heterogeneous turbid media: Analytic solutions and applications," *Appl. Opt.*, vol. 35, pp. 3746–3758 (1996).
- [2] M.J. Eppstein, D.J. Hawrysz, A. Godavarty, and E.M. Sevick-Muraca, "Three-dimensional, Bayesian image reconstruction from sparse and noisy data sets: near-infrared fluorescence tomography," *P. Natl. A. Sci. USA*, vol. 99, pp. 9619–9624, 2002.
- [3] A.D. Klose and A.H. Hielscher, "Fluorescence tomography with simulated data based on the equation of radiative transfer," *Opt. Lett.*, vol. 28, pp. 1019–1021, 2003.
- [4] A.B. Milstein, *et al.* "Fluorescence optical diffusion tomography," *Appl. Opt.*, vol. 42, pp. 3081–3094, 2003.
- [5] V. Ntziachristos and R. Weissleder, "Experimental three-dimensional fluorescence reconstruction of diffuse media using a normalized Born approximation," *Opt. Lett.*, vol. 26, pp. 893–895, 2001.
- [6] R.B. Schulz, J. Ripoll, and V. Ntziachristos, "Noncontact optical tomography of turbid media," *Opt. Lett.*, vol. 28, pp. 1701–1703 2003.
- [7] R.B. Schulz, J. Ripoll, and V. Ntziachristos, "Experimental fluorescence tomography of tissues with noncontact measurements," *IEEE Trans. Medical Imaging*, vol. 23, pp. 492–500, 2004.
- [8] H. Meyer, A. Garofalakis, G. Zacharakis, E. Economou, C. Mamalaki, D. Kioussis, V. Ntziachristos, and J. Ripoll, "A multi-projection non-contact fluorescence tomography setup for imaging arbitrary geometries," presented at the 2005 Optical Tomography and Spectroscopy of Tissue VI Proceedings of SPIE.
- [9] A. Molins, A. Soubret, and V. Ntziachristos, "Complete angle projection fluorescent tomography of tissues," presented at the 27th Annual International Conference of the IEEE Engineering in Medicine and Biology Society, Shanghai, China, Sep. 1–4, 2005.
- [10] X. Intes, *et al.*, "Projection access order in algebraic reconstruction technique for diffuse optical tomography," *Phys. Med. Biol.*, vol. 47, N1–N10, Jan 2002.
- [11] M. Potmesil, "Generating octree models of 3D objects from their silhouettes in a sequence of images", *Comp. Vis. Graph. Img. Proc.*, vol. 40, 1–29, 1987.
- [12] A. Laurentini, "The Visual Hull: A new tool for contour-based image understanding," in *Proc. 7th Scandinavian Conf. Image Analysis*, Aalborg, Denmark, 1991, pp. 993–1002.
- [13] W.E. Lorensen and H.E. Cline, "Marching cubes: A high resolution 3D surface construction algorithm," in *Proc. 14th Int. Conf. on Computer Graphics and Interactive Techniques*, New York: Association for Computing Machinery, 1987, pp. 163–169.
- [14] G. Zacharakis, J. Ripoll, R. Weissleder, and V. Ntziachristos, "Fluorescent protein tomography scanner for small animal imaging," *IEEE Trans. Medical Imaging*, vol. 24, pp. 878–885, July 2005.
- [15] T. Lasser and V. Ntziachristos, "Surface Reconstruction from Contours for Non-contact Fluorescence Molecular Tomography," presented at the 2006 *OSA Biomedical Optics Topical Meeting*, Fort Lauderdale, FL, March 19–23, 2006, SH37.